

**Selective excitation of exciton transitions in PTCDA crystals and films**V. R. Gangilenka, L. V. Titova,\* L. M. Smith, and H. P. Wagner  
*Department of Physics, University of Cincinnati, Cincinnati, Ohio 45221-0011, USA*L. A. A. DeSilva  
*Department of Physics & Geology, Northern Kentucky University, Highland Heights, Kentucky 41099, USA*L. Gisslén and R. Scholz  
*Walter Schottky Institut und Physik Department, Technische Universität München, 85748 Garching, Germany*  
(Received 6 May 2009; revised manuscript received 6 January 2010; published 19 April 2010)

Photoluminescence excitation studies on 3,4,9,10-perylene tetracarboxylic dianhydride (PTCDA) single crystals and polycrystalline PTCDA films are compared to the calculated excitonic dispersion deduced from an exciton model including the coupling between Frenkel and charge transfer (CT) excitons along the stacking direction. For excitation energies below the 0-0 Frenkel exciton absorption band at 5 K these measurements enable the selective excitation of several CT states. The CT2 state involving stacked PTCDA molecules reveals two excitation resonances originating from different vibronic sublevels. Moreover, the fundamental transition of the CT1 exciton state delocalized over both basis molecules in the crystal unit cell has been identified from the corresponding excitation resonance. From the excitation energy dependence the fundamental transition energies of the CT2 and CT1 excitons have been deduced to occur at 1.95 and 1.98 eV, respectively. When the excitation energy exceeds  $\sim 2.08$  eV, we observe a strong emission channel which is related to the indirect minimum of the lowest dispersion branch dominated by Frenkel excitons. Photoluminescence excitation spectroscopy measurements on polycrystalline PTCDA films reveal a strong CT2 signal intensity which is attributed to an increased density of defect-related CT2 states that are preferentially formed by slightly deformed or compressed stacked PTCDA molecules in the vicinity of defects or at grain boundaries. Temperature-dependent PL measurements in polycrystalline PTCDA films between 10 and 300 K at an excitation of 1.88 eV further allow a detailed investigation of the CT2 transition and its vibronic subband.

DOI: [10.1103/PhysRevB.81.155208](https://doi.org/10.1103/PhysRevB.81.155208)

PACS number(s): 78.55.Kz, 78.20.Bh, 71.35.Aa

**I. INTRODUCTION**

The physical origin of the excitonic emission in polycrystalline molecular films and in polymers has been the subject of intense research for more than 20 years. In this context, photoluminescence excitation (PLE) spectroscopy has become a powerful optical technique allowing to establish a correspondence between specific absorption resonances and the resulting radiative recombination channels. For twisted molecules such as parahexaphenyl and various conjugated polymers, PLE has demonstrated a dependence of the PL bands on the excitation energy. When exciting above a certain threshold energy the shape of the PL bands does not depend on the excitation energy but below this threshold they follow the excitation energy with a constant Stokes shift.<sup>1-4</sup> This finding has been interpreted as a consequence of an inhomogeneously broadened distribution of transition energies. Excitation at sufficiently high energy allows the exciton to migrate to any other site before eventually emitting a PL photon. Excitation into the lower part of the distribution addresses specific sites with low transition energies so that the exciton remains in the same spatial region before eventually emitting in the red edge of the inhomogeneously broadened PL band. This corresponds to a redshift with respect to the entire distribution of recombination energies which would become available when exciting above the threshold energy. Therefore, this threshold is interpreted as a localization energy defining the demarcation line between high-energy excitons migrating between sites and low-

energy excitons remaining confined in the spatial region where they have been excited.<sup>2</sup>

In polymers, the typical conjugation length between kinks along the chain and the twisting angles between adjacent chromophores are not predetermined by the molecular structure but they result merely from the geometric conformation realized in an amorphous assembly. Together with the energetic influence of the random arrangement between neighboring chains, the dependence of the transition energy on the conjugation length and on the twisting angles defines obvious microscopic reasons for an inhomogeneously broadened distribution of transition energies.<sup>1</sup> In more regular compounds such as parahexaphenyl, the chain length is fixed. Nevertheless, deviations from planarity still produce a rather broad distribution over transition energies, resulting again in a localization threshold.<sup>2</sup>

For more rigid compounds such as perylene-based chromophores and pentacene, a variation in the conjugation length or an internal twisting of the molecule can be excluded as a source of inhomogeneous broadening. Instead, librational phonon modes are strongly elongated by optical excitations, resulting eventually in a pronounced Raman activity and correspondingly to rather broad absorption features.<sup>5-7</sup> Therefore, several mechanisms that are responsible for spectral diffusion in other organic materials should not be present in perylene-based chromophores resulting in a reduced spectral diffusion.

Among these materials, the emission from molecular 3,4,9,10-perylene tetracarboxylic dianhydride (PTCDA)

single crystals and polycrystalline films shows a particularly rich variety of excitonic bands at low temperatures (10–100 K) (Refs. 8–16) and the identification of these recombination channels is still subject of intense debate. In the present work, we apply PLE to this compound allowing to confirm previous assignments of the various PL channels by identifying the respective PLE resonances.

This work is organized as follows. Section II summarizes previous PL and PLE studies of PTCDA single crystals and polycrystalline thin films. In Sec. III, as a theoretical background for the subsequent assignment of the PL channels and the corresponding PLE resonances, we discuss the excitonic dispersion arising from a model based on Frenkel excitons and CT states involving stack neighbors.<sup>17</sup> Section IV is devoted to the experimental setup and Sec. V presents PLE spectra obtained from PTCDA single crystals and from polycrystalline PTCDA films.

## II. PREVIOUS PL AND PLE STUDIES ON PTCDA

PTCDA forms polycrystalline films in the monoclinic space group  $P2_1/c$  with two different modifications (the  $\alpha$  and  $\beta$  phase),<sup>18</sup> both possessing two nearly coplanar molecules in the crystal unit cell.<sup>9</sup> The molecules are aligned parallel to the (102) lattice plane which coincides with the substrate surface. The distance between consecutive molecular planes along the  $\mathbf{a}$  lattice vector is shorter than in graphite, resulting in a large overlap of molecular  $\pi$  orbitals. Accordingly, early PL investigations at low temperatures<sup>8,9</sup> assign the high energy emission to Frenkel exciton transitions and attribute emission bands at lower energy to nonrelaxed as well as to self-trapped charge transfer (CT) excitons. Several theoretical models that include Frenkel excitons, CT excitons, and self-trapped excitons<sup>19–22</sup> have been developed to describe and support the experimental observations.

More recent investigations use time-resolved PL (TRPL) measurements on  $\alpha$ -PTCDA single crystals and on polycrystalline films to differentiate various recombination channels.<sup>12–14,16</sup> The TRPL studies were performed in the temperature range from 10 to 300 K. From the recombination times that were detected within the emission band, five different exciton emission channels have been isolated at low temperature:<sup>12,14</sup> (1) a high-energy emission band due to a nonrelaxed charge-transfer transition (CT2-nr) between two PTCDA molecules stacked along the  $\mathbf{a}$  direction at 1.95 eV, (2) vertical recombination from an indirect minimum of the lowest dispersion branch of the Frenkel exciton giving an emission maximum at  $\sim 1.82$  eV, (3) a relaxed charge-transfer transition between two PTCDA basis molecules within the same unit cell (CT1) with a peak energy at  $\sim 1.85$  eV, (4) a self-trapped CT2 exciton involving a reduced distance between stacked PTCDA molecules with peak energy at  $\sim 1.71$  eV, and (5) the respective excimer transition with a PL maximum at  $\sim 1.76$  eV which is weak at low temperature but becomes the dominant band at higher temperatures ( $T > 200$  K). These band assignments are supported by recent PL measurements under uniaxial pressure.<sup>23</sup> With increasing pressure, the CT2 gains intensity relative to the Frenkel exciton emission, and the CT2 transition reveals

a shift to lower energies. Both observations are attributed to an increased exciton trapping probability and to an enhanced Coulomb attraction at a reduced distance between oppositely charged stacked molecules. These interpretations as well as the above-mentioned band assignments are further supported by theoretical models that handle pure Frenkel exciton transitions<sup>24–28</sup> and CT states separately.<sup>29</sup>

In addition to the PL investigations, only a few studies have applied the technique of PLE to PTCDA films,<sup>11,15</sup> using a tunable excitation source covering the PTCDA absorption band from  $\sim 2.0$  up to  $\sim 3.0$  eV. The change in the PLE signal as a function of the substrate temperature<sup>11</sup> and of the growth temperature<sup>15</sup> of deposited films was used to study the influence of the  $\alpha$ - and  $\beta$ -phase growth morphology on the optical properties rather than to identify different PL lines according to their electronic nature. In particular, investigations on PTCDA films deposited on different substrates such as quartz, KCl, and NaCl attribute the energy band at  $\sim 1.85$  eV (Y-line) to the  $\beta$  phase of PTCDA, whereas the low-energy band at  $\sim 1.71$  eV (E-band) is assigned to the  $\alpha$  phase.<sup>11</sup> More recent investigations on PTCDA films deposited on Ag(111) (Ref. 15) at different growth temperatures reveal a weak dependence of the Y-line on the PTCDA growth morphology whereas the E-band shows an intensity maximum in a temperature regime where the  $\alpha$  and  $\beta$  phase coexist. Accordingly, the E-band is attributed to excimerlike states that are preferentially formed at stacking defects in PTCDA layers.

In this work, using  $\alpha$ -PTCDA single crystals and polycrystalline films grown on naturally oxidized Si(100) substrate, we performed PLE measurements at low temperature where the optical excitation energy was varied *below* the 0-0 Frenkel exciton absorption band. This range of excitation energies allows the selective excitation of Frenkel excitons as well as of various CT excitons. Our interpretation of the PLE data is based on existing calculations concerning the dispersion of pure Frenkel excitons<sup>25</sup> and investigations of PL from self-trapped CT excitons involving two stack neighbors at reduced intermolecular distance.<sup>29</sup> Recently, an exciton model including the mixing between Frenkel excitons and CT states via electron transfer and hole transfer has been applied to the optical properties of six perylene pigments including PTCDA.<sup>17</sup> In the present work, this model is applied to an assignment of the PLE resonances and the excitonic dispersion derived from the same Hamiltonian is presented here, corroborating previous assignments of the various radiative recombination channels.

## III. EXCITONIC DISPERSION

The exciton model discussed in the following paragraph includes neutral molecular excitations and CT transitions between stack neighbors, called CT2 throughout the remaining parts of this work. Both kinds of excitations are coupled by electron transfer  $t_e$  and hole transfer  $t_h$  along the stacking direction  $\mathbf{a}$  via off-diagonal matrix elements  $t'_h e^{ik \cdot \mathbf{a}} + t'_e$  where  $t'_h$  and  $t'_e$  are the fermionic transfer parameters modified by Franck-Condon factors, and  $\mathbf{k}$  is the wave vector of an excitonic Bloch wave, compare Ref. 17 for further details. In

contrast to the pioneering work using empirical parameters,<sup>20</sup> this exciton model is based on calculated values for the intermolecular electron and hole transfer obtained with density-functional theory (DFT). It also includes reorganization energies computed with DFT in the form of a progression over an effective internal vibration  $\hbar\omega$  with a Huang-Rhys factor  $S$ , and transition dipoles of the CT states derived from time-dependent DFT.<sup>17</sup>

Due to momentum conservation, the small wave vector of the photon results in an excitonic Bloch wave close to the  $\Gamma$  point of the Brillouin zone, corresponding to  $\mathbf{k}=0$ . For this particular wave vector, electron and hole transfer interfere constructively according to  $t'_h+t'_e$ , but for PTCDA with its nearly parallel valence and conduction bands,  $t_e$  and  $t_h$  have opposite signs, so that their contribution of the Frenkel-CT mixing to the second moment of the absorption band according to  $(\Delta E)^2=S(\hbar\omega)^2+2(t_e+t_h)^2$  remains much smaller than the second moment of the Poisson progression over the effective internal mode,  $S(\hbar\omega)^2$ . In the calculation of the optical line shape, the energy of a CT2 state involving two stacked molecules in the undeformed crystal remains the only relevant fitting parameter required for an optimum agreement with the observed optical response.<sup>30-32</sup>

The comparison of this model with the dielectric tensor of  $\alpha$ -PTCDA single crystals obtained at room temperature provides values of  $E_{00}^F=2.17$  eV and  $E_{00}^{CT2}=1.95\pm 0.07$  eV for the fundamental 0-0 transitions of the neutral molecular excitation and of charge transfer along the stack, respectively.<sup>17</sup> Due to the particularly small mixing between Frenkel excitons and CT2 states via electron transfer  $t_e$  and hole transfer  $t_h$  according to  $t_e+t_h=-10$  meV, the influence of the CT2 state on the linear optical properties remains rather small so that a comparison between calculated and observed spectra does not allow for a more precise determination of the CT2 transition energy.

From temperature-dependent investigations of PTCDA and several other perylene compounds it can be estimated that the stacking vector of PTCDA is reduced by about 1.5% at low temperatures resulting in a redshift of the absorption band by about 0.02 eV.<sup>14,33,34</sup> Assuming that the CT2 transition shifts by the same amount, this would place the fundamental transitions at  $E_{00}^F=2.15$  eV and  $E_{00}^{CT2}=1.93\pm 0.07$  eV. For reasons which will become clear in the subsequent parts of this work, we choose a slightly higher value of  $E_{00}^{CT2}=1.95$  eV for the CT2 transition along the stack, still within the conservative uncertainty range derived from the comparison between the calculated dielectric tensor and the observed values deduced from spectroscopic ellipsometry.<sup>32</sup>

With these ingredients, the previous calculation of the excitonic states in the center of the Brillouin zone can easily be generalized to finite wave vectors. Figure 1 shows the calculated excitonic dispersion branches at low temperatures, where the resulting optical properties derived from the dipole-allowed states at  $\Gamma$  are again in good agreement with the observed spectra.<sup>28,35</sup> The topmost branches with a large Frenkel exciton parentage are shown as thicker lines and their pair with maxima around 2.20 and 2.22 eV can be analyzed further in terms of the Davydov splitting between the lowest strong absorption peaks occurring for orthogonal

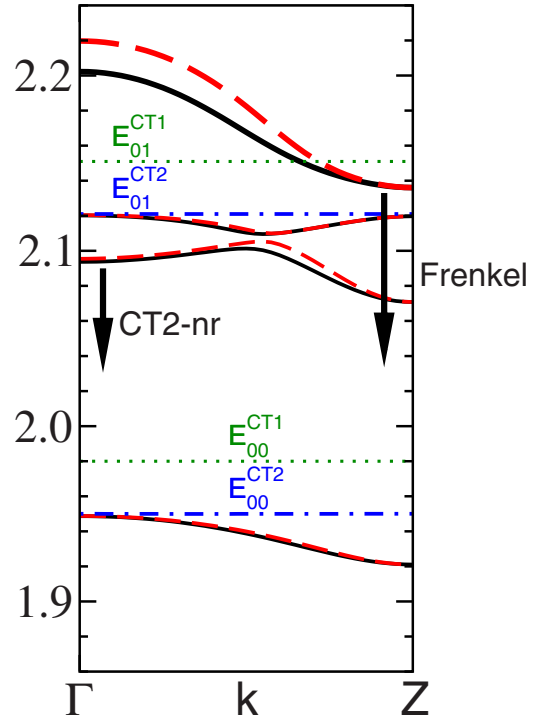


FIG. 1. (Color online) Exciton dispersion in  $\alpha$ -PTCDA at low temperature. Blue dash-dotted: dipole-forbidden vibronic levels of CT2 exciton involving stack neighbors; black, red dashed: dispersion branches of dipole-allowed mixed Frenkel-CT2 states, black for light polarized along  $x$  direction (in  $ac$  plane) and red dashed for light polarized along  $y$  direction (parallel to  $b$  lattice vector); green dotted: vibronic levels of CT1 exciton involving both basis molecules.

polarizations.<sup>17,32</sup> Moreover, the minima of these dispersion branches at the surface of the Brillouin zone close to 2.14 eV give rise to vertical radiative recombination to excited vibronic levels of the effective internal vibration, as indicated by the arrow.<sup>25,26</sup> Due to the low-lying CT transitions, several excitation resonances below the lowest Frenkel dispersion branch are worth mentioning: The fundamental  $E_{00}^{CT2}=1.95$  eV for charge transfer along the stack, the region between 2.10 and 2.12 eV dominated by the first vibronic level of the CT2 manifold at  $E_{01}^{CT2}=2.12$  eV and the fundamental  $E_{00}^{CT1}=1.98$  eV for charge transfer between the two basis molecules in the crystal unit cell. As the electron or hole transfer between the two basis molecules is expected to be smaller than the respective transfers along the stack, the CT1 states are not included in the exciton model, so that their dispersion branches are visualized by horizontal lines. From the PLE spectra discussed below, a suitable CT1 energy in the crystal can be obtained, as shown in Fig. 1. Residual deviations between the calculated excitation resonances in Fig. 1 and the PL peaks obtained for samples cooled to a temperature of 5 K will be discussed in Sec. V.

#### IV. SAMPLES AND EXPERIMENTAL SETUP

##### A. Samples

The  $\alpha$ -PTCDA single crystals analyzed in the present work were grown by sublimation under high vacuum



( $10^{-6}$  mbar) from source material (Sigma Aldrich) at a temperature of 300 °C. The samples were in the form of needles, typically  $50 \times 50 \mu\text{m}^2$  in cross section and 2 mm in length. Their crystalline phase has been determined by x-ray diffraction to be the  $\alpha$ -monoclinic variety. The PTCDA films investigated in the following had thicknesses of about 90 and 50 nm. They were grown by organic molecular-beam deposition (OMBD) onto chemically clean *n*-type (100) oriented naturally oxidized Si. The substrates were cleaned in an ultrasonic bath using acetone, methanol, and ultrapure water. Then they were transferred into the high-vacuum OMBD chamber with a base pressure of  $10^{-8}$  mbar. The PTCDA source material (Sigma Aldrich) was purified by sublimation at a temperature of 300 °C before it was filled into the Knudsen cell. During growth the deposition rate was measured using a quartz crystal-thickness monitor that was calibrated by different film-thickness measurements using a profilometer, optical ellipsometry, and absorption measurements. Typical deposition rates on substrates held at room temperature were 0.01 nm/s when the effusion cells were heated to 320 °C. X-ray diffraction measurements in  $\theta$ - $2\theta$  scan mode at room temperature reveal an  $\alpha/\beta$ -PTCDA ratio of better than 40:1 and a full width at half maximum (FWHM) of  $0.37^\circ$  for the  $\alpha$ -PTCDA reflex at  $2\theta = 27.81^\circ$ .<sup>14</sup>

### B. Optical instrumentation

For the PLE measurements an Ar-ion laser ( $\lambda = 514$  nm) pumped dye laser was used as variable excitation source. Two dyes, DCM (4-dicyanomethylene-2-methyl-6-p-dimethylamino-styryl-4H-pyran) as well as Rhodamine 6G, were used in order to cover the energy range from 1.88 to 2.15 eV. The PTCDA samples were mounted in a continuous flow He cryostat and kept at a temperature of 5 K. The laser beam was focused onto the PTCDA crystal and the PTCDA film, respectively, with a  $50\times$  microscope objective lens resulting in a laser spot diameter of  $\sim 2 \mu\text{m}$  on the sample. The excitation power was of the order of 100  $\mu\text{W}$  at the sample position. The PL from the PTCDA samples was collected with the same objective lens, directed through a dichroic mirror and dispersed by a Dilor spectrometer. Finally, the PL signal was detected by a nitrogen-cooled charge coupled device array. For the PTCDA polycrystalline films GaAs-based semiconductor lasers emitting at 660 nm ( $\sim 1.88$  eV) and 692 nm ( $\sim 1.79$  eV) were used as additional excitation sources. The laser beam had a diameter of  $\sim 200 \mu\text{m}$  on the sample, the excitation power was  $\sim 5$  mW at the PTCDA sample position. The emitted PL was analyzed by a grating monochromator and a GaAs photomultiplier. A closed-cycle He cryostat was used in these measurements to provide a variable temperature between 10 and 300 K.

## V. EXPERIMENTAL RESULTS AND DISCUSSION

### A. PTCDA single crystals

Figure 2 shows the PL spectra of a PTCDA single crystal at 5 K at various excitation energies ranging from 1.878 to 2.149 eV and at a laser power of 100  $\mu\text{W}$ . For better visibility the spectra at low-excitation energies (1.878–1.937

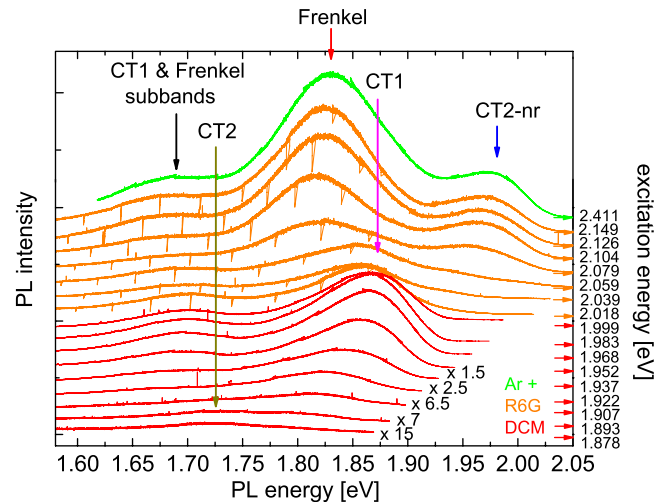


FIG. 2. (Color online) PL excitation spectra of a PTCDA single crystal at 5 K at excitation energies ranging from 1.878 to 2.149 eV using DCM and Rhodamine 6G dye lasers as labeled. The topmost spectrum is excited with an Ar ion laser at an excitation energy of 2.411 eV. The PL spectra are offset to each other for clarity and the weakest spectra at low-excitation energy are multiplied by different magnification factors as labeled.

eV) are multiplied by scaling factors as labeled. In addition the spectra are offset to each other for clarity. Furthermore, a PL spectrum excited at 2.411 eV (Ar-ion laser line) is given for comparison.

At the lowest-excitation energy (1.878 eV) a broad emission band with a peak energy at 1.72 eV can be weakly excited. The PL band energy is close to the self-trapped CT2 transition energy identified by time-resolved PL measurements on PTCDA crystals at low temperatures.<sup>12,13</sup> We therefore attribute this emission band to self-trapped CT2 excitons between oppositely charged stacked PTCDA molecules at a reduced distance. As their excitation energy of 1.878 eV is significantly less than the 0-0 transition energy of the CT2 exciton at 1.95 eV (see Fig. 1) we assume that this excitation occurs at a specific defect, presumably a dislocation at a grain boundary, or in a strongly strained region close to such a defect favoring charge separation into anion-cation pairs. This defect-related CT2 resonance shows a weak intensity maximum at an excitation of 1.893 eV and starts to decrease at higher excitation energies up to 1.92 eV.

However, at slightly higher excitation energies, a second narrower and strong PL band with rapidly increasing intensity emerges at energies above 1.8 eV which may hide a further contribution of the CT2 resonance to the observed spectra. With increasing excitation energy, the center energy of this band shifts linearly to higher values and reaches a constant value ( $\sim 1.86$  eV) at excitation energies larger than 1.968 eV. By comparison with earlier investigations<sup>12,13</sup> we assign this emission band to the relaxed CT1 transition between PTCDA molecules within the same unit cell. In addition a weaker emission band appears in the PL spectra, separated from the CT1 band by  $\sim 160$  meV to lower energy. This weak PL band shows the same excitation-energy dependence as the CT1 emission. Accordingly, it is attributed to the first vibronic subband of the CT1 transition where the

energy difference of  $\sim 160$  meV corresponds to the effective internal vibrational mode of the molecule of about 170 meV.<sup>8,17,20</sup> Previous microelectronic calculations find an energy difference  $E(\text{CT1}) - E(\text{CT2})$  of 0.60 eV (Ref. 36) or of  $-30$  to  $-100$  meV,<sup>37</sup> depending on the method used for the assignment of charges to different subgroups of a PTCDA molecule. With respect to this large scatter among different theoretical predictions, the PLE spectra allow a particularly precise determination of this energetic difference.

Above 2.018 eV excitation energy, the CT1 emission decreases, and two new PL bands appear at  $\sim 1.79$  and at  $\sim 1.92$  eV, respectively. With increasing excitation energy the intensities of both bands increase rapidly. The emission at  $\sim 1.92$  eV shows a blueshift with increasing excitation energy similar to that of the CT1 transition and of its vibronic subband at lower energy. The 1.79 eV emission band also shifts to higher energy but with a significantly lower rate. When the excitation energy exceeds  $\sim 2.126$  eV, these PL bands reach transition energies of  $\sim 1.82$  and  $\sim 1.97$  eV, respectively. An excitation up to 2.411 eV (Ar laser line) does not lead to considerable further changes in the PL emission spectrum.

Furthermore, the intensity of the high-energy band starts to saturate while the intensity of the 1.82 eV band still rises with increasing excitation energy. By comparison with the topmost spectrum that was taken at an excitation energy of 2.411 eV (Ar-ion laser), thus well above the  $|0_g\rangle \rightarrow |0_e\rangle$  (0-0) Frenkel exciton absorption band at  $\sim 2.21$  eV at  $\mathbf{k}=0$ ,<sup>24,25,28</sup> it becomes obvious that the strong emission band at 1.82 eV is due to the indirect  $|0_e\rangle \rightarrow |1_g\rangle$  Frenkel exciton transition.<sup>12,13</sup> By comparison with earlier investigations on PTCDA films and with recent model calculations (see Fig. 1), the high-energy band at 1.97 eV emission energy is attributed to the vertical recombination of a mixed Frenkel-CT transition (which is called CT2-nr) involving the first vibronic level of the CT2 manifold.<sup>14</sup>

Figures 3 and 4 summarize the shifts of the spectral positions and the PL intensities (Gaussian areas) of the different recombination channels, respectively, as a function of the excitation energy ranging from 1.878 to 2.149 eV. For comparison the dashed-red line in Fig. 3 is showing the position of emission resonant with the excitation energy. The center energies  $E_j$  and the Gaussian areas  $a_j$  of the emission bands were deduced from Fig. 2 using a multi-Gaussian approximation where each observable recombination channel ( $j=\text{CT1}$ -subband, CT1, CT2, Frenkel exciton, and CT2-nr, respectively) was expressed by one adjustable Gaussian function

$$I_{\text{PL}}(E) \propto E^3 \sum_j \frac{a_j}{\sigma_j \sqrt{2\pi}} \exp \left[ -\frac{1}{2} \left( \frac{E - E_j}{\sigma_j} \right)^2 \right]. \quad (1)$$

Above an excitation of 2.018 eV the spectral position and the FWHM  $\sqrt{8 \ln 2} \sigma_j$  of the CT1 Gaussian were kept fixed at 1.857 eV and 90 meV, respectively, in order to obtain a better accuracy of the energies and Gaussian areas of the other emission bands. In addition, Fig. 4 comprises the absorption spectrum  $\alpha(\omega)$  of PTCDA at 10 K as a black solid line. The absorption curve has been calculated from the optical density

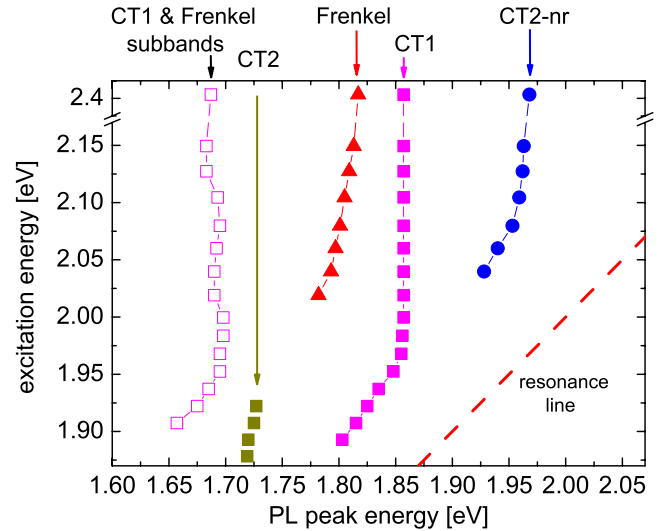


FIG. 3. (Color online) Different exciton emission channels in a PTCDA crystal at 5 K as a function of the excitation energy ranging from 1.878 to 2.149 eV. The emission channels are obtained from the spectra in Fig. 2 by a multi-Gaussian decomposition of the observed line shape as described in the text. The dashed-red line is showing the position of emission resonant with the excitation energy.

of a 36-nm-thick PTCDA film on Pyrex obtained from transmission measurements at 10 K.<sup>28</sup> For these calculations a Kramers-Kronig consistent model for the refractive index with an extinction coefficient  $\Im[n(\omega)]$  defined as a sum of Gaussians has been used. In contrast to the measured optical density (see Ref. 28), in the absorption coefficient  $\alpha(\omega) = 2 \frac{\omega}{c} \Im[n(\omega)]$  reflectivity losses at the PTCDA/air and PTCDA/Pyrex interfaces have been eliminated so that it

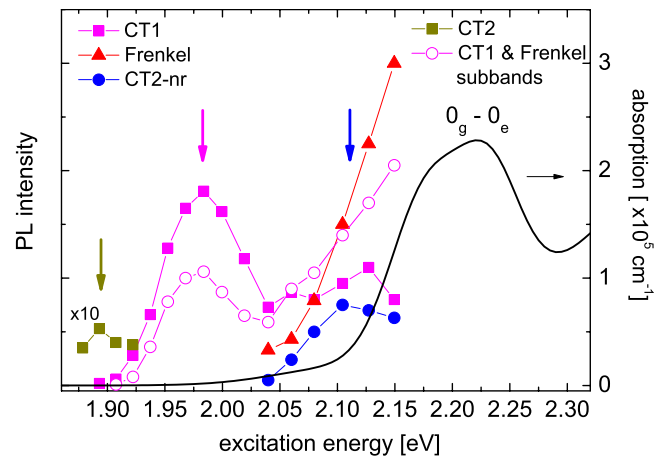


FIG. 4. (Color online) PL intensity (Gaussian areas) of different emission channels in PTCDA crystals at 5 K as a function of the excitation energy ranging from 1.878 to 2.149 eV obtained from the spectra in Fig. 2. Arrows indicate the energy positions of the distribution maxima of CT2, CT1, and CT2-nr states, respectively. In addition an absorption curve derived from the optical density of a 36-nm-thick PTCDA film on Pyrex at 10 K using a Kramers-Kronig consistent model for the complex refractive index is shown as black solid line.

shows a steeper energy dependence below the  $0_g-0_e$  Frenkel exciton transition.<sup>28</sup>

Figure 3 clearly reveals a blueshift of the CT1 emission and its vibronic subband when the laser starts to excite the low-energy side of the inhomogeneously broadened distribution of CT1 states. Since the density of these low-energy states is small, the PL intensity is initially weak but rapidly grows with increasing excitation energy due to the rising number of accessible states revealing an emission peak at 1.98 eV at the maximum of the CT1 state density. Compared to PLE studies on compounds where deviations from planarity contribute to a redshift of the PL spectra following the laser line,<sup>1</sup> in PTCDA this redshift can only be observed within a rather narrow energetic range of  $\sim 0.05$  eV. This finding supports our previous statement that several of the mechanisms contributing to spectral diffusion in more disordered molecular assemblies are not present in PTCDA. Local strain effects around defects such as stacking faults emerge as the most likely origin being responsible for the remaining spectral diffusion in highly ordered molecular crystals consisting of planar molecules. Accordingly, the optically excited states start to relax into energetically lower lying states when the laser excitation exceeds the maximum of the CT1 distribution, showing an excitation-energy-independent emission at center energies of  $\sim 1.86$  and  $\sim 1.70$  eV for the CT1 transition and its vibronic subband, respectively. Since the density of states decreases at energies above the maximum of the CT state distribution, the PL intensity of the CT1 transition and its vibronic subband decreases for excitation energies higher than 1.983 eV (see Fig. 4). The energy difference of  $\sim 120$  meV between the CT1 absorption maximum ( $\sim 1.98$  eV) and the PL peak ( $\sim 1.86$  eV) is in good agreement with the 110 meV Stokes shift caused by low-frequency internal breathing and external phonon modes as discussed earlier.<sup>26,27</sup> For excitation into the lower edge of the CT1 distribution the Stokes shift is reduced by up to 20 meV.

As shown in Fig. 4, the PL intensity of the weak CT2 transition at  $\sim 1.72$  eV shows a weak maximum at an excitation energy of 1.893 eV. With increasing excitation energy the CT2 PL intensity slightly drops while the center energy of the inhomogeneously broadened band remains constant, indicating that the laser energy already exceeds the maximum of the density of states of an absorption resonance. At the lowest-excitation energy (1.878 eV) the CT2 PL intensity is reduced due to the decrease in available charge transfer states that can be excited. Investigations on PTCDA films with excitation energies below 1.878 eV presented in Sec. VB show a more pronounced reduction in the PL intensity with decreasing excitation energy confirming this interpretation.

The energy difference of  $\sim 175$  meV between the defect-related CT2 absorption maximum ( $\sim 1.893$  eV) and the PL peak ( $\sim 1.72$ ) is significantly larger than the expected 110 meV Stokes shift caused by the low-frequency modes.<sup>26,27</sup> The remaining energy of  $\sim 65$  meV, however, can be explained by the self-trapping of the anion-cation pair along the molecular stacking direction. The respective contribution to the Stokes shift has been calculated by a combination of a Møller-Plesset- (MP2-) based intermolecular van der Waals

potential and configuration interaction of singly excited states for the CT2 transition, resulting in an additional redshift of 0.07 eV which is in good agreement with the value deduced from PLE.<sup>29</sup>

For energies larger than  $\sim 2.04$  eV the indirect Frenkel exciton and the CT2-nr start to occur in the PL spectra. As demonstrated earlier, the radiative lifetime of about  $12.7 \pm 0.4$  ns for the emission from the minimum of the Frenkel exciton dispersion and the two decay times of  $3 \pm 1$  and  $33.5 \pm 2$  ns assigned to the CT2-nr PL band are incompatible, excluding a common radiative precursor state. While the CT2-nr transition energy shows a similar dependence as the CT1 transition for laser energies that are below the maximum of the state distribution, the Frenkel exciton transition reveals an unexpectedly weak excitation energy dependence (see Fig. 2). Although the optical excitation energies are significantly lower than the  $|0_g\rangle \rightarrow |0_e\rangle$  absorption energy of  $\sim 2.21$  eV (Refs. 24, 25, and 28) the relaxed Frenkel exciton-transition energy reached its final value of 1.82 eV already at  $\sim 2.15$  eV excitation energy. According to model calculations of the excitonic dispersion summarized in Sec. III,<sup>17,38</sup> the minimum of the lowest-dispersion branch dominated by Frenkel excitons at the surface of the Brillouin zone occurs about 70 meV below the dispersion maxima at  $\Gamma$ .<sup>25,27</sup> After thermal relaxation into this energetic minimum the lowest accessible final state for recombining excitons is the  $|1_g\rangle$  state which lowers the transition energy by about 170 meV, corresponding to the energy of an effective internal vibration. The PL energy from this dispersion minimum is further reduced by about 110 meV caused by low-frequency modes<sup>26,27</sup> resulting in a total Stokes shift of  $\sim 0.39$  eV for optical excitation resonant to the 0-0 dispersion branch of the Frenkel exciton at the  $\Gamma$  point. Even at the highest excitation energy of  $\sim 2.15$  eV in our PLE measurements, the expected Stokes shift of the Frenkel exciton emission amounts to only 0.33 eV. Therefore, opposite to the CT transitions at lower energies, an excitation into the low-energy edge of the 0-0 Frenkel resonance at 2.15 eV allows the observation of the entire density of states of the respective PL channel. On the other hand, at energies ranging from  $\sim 2.05$  to 2.15 eV, the PL from Frenkel excitons shows a redshift similar to the excitation of CT states below their absorption resonance. We therefore suggest that in this energetic range, the observed Frenkel exciton PL band is generated by selective excitation of spatial regions with a particularly low-lying transition energy, e.g., due to compressive strain.<sup>23</sup>

Moreover, in this energetic region, excitation into the mixed Frenkel-CT2 states which are dominated by  $E_{01}^{CT2}$  basis states at 2.10 and 2.12 eV might also contribute to an emission from the dispersion minimum of the lowest branch dominated by Frenkel excitons at 2.14 eV. On a first sight, at a temperature as low as  $T=5$  K, scattering from a mixed Frenkel-CT2 state absorbing around 2.10 or 2.12 eV into a dispersion minimum at 2.14 eV seems to be energetically unfavorable. However, considering the Stokes shift of low-frequency vibrations and external phonons the emission occurs from excitonic states about 110 meV lower in energy than the respective dispersion minimum in Fig. 1 calculated for the equilibrium geometry of the undeformed crystal, or at  $\sim 2.03$  eV.



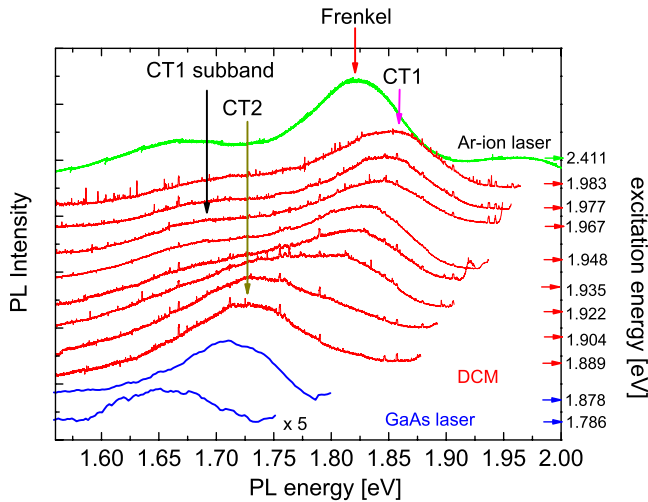


FIG. 5. (Color online) PL spectra of a 90-nm-thick PTCDA film on Si substrate at 5 K as a function of the excitation energy ranging from 1.889 to 1.983 eV using a DCM dye laser. The topmost spectrum is excited with an Ar ion laser at an excitation energy of 2.411 eV. The two bottommost PLE spectra are excited with GaAs semiconductor lasers at 1.878 and 1.786 eV. For easier comparison the PL spectra are offset to each other.

As shown in Fig. 4 this Frenkel contribution increases significantly at higher excitation energy, leading to a strong enhancement of the PL signal (Gaussian area) at  $\sim 1.83$  eV and of the PL band at  $\sim 160$  meV lower in energy. While the latter band has been attributed exclusively to the CT1-subband below an excitation energy of 2.08 eV, it now increasingly contains the vibronic subband of the Frenkel exciton, resulting in a larger FWHM of this band as well as in a slight shift to lower energy at higher excitation energies.

As discussed in Sec. III the first vibronic level of the CT2 manifold at  $E_{01}^{\text{CT2}} = 2.12$  eV or more specifically the mixed Frenkel-CT2 state at 2.10 eV is the relevant excitation channel resulting in the CT2-nr PL band occurring at a constant emission energy of  $\sim 1.97$  eV for excitation energies above  $\sim 2.10$  eV.<sup>26,27</sup> As for the relaxed CT2 transition, the observed Stokes shift of  $\sim 130$  meV exceeds the shift of  $\sim 110$  meV expected from low-energy modes. The PLE resonance around 2.10 eV assigned to the mixed Frenkel-CT2 dispersion branch coincides with a PLE resonance and a peak in photocurrent measurements reported earlier.<sup>8,39</sup> This indicates that an excitation into the mixed Frenkel-CT2 states favors the decomposition of the exciton into an electron-hole pair contributing to the photocurrent. The more strongly absorbing Frenkel part of this mixed exciton gives the main contribution to the transition dipole required for the absorption process preceding the charge separation.<sup>17</sup>

In contrast to the Frenkel exciton band the CT2-nr band does not further increase its Gaussian area for excitation above  $\sim 2.10$  eV, indicating that the distribution maximum of these states has been reached by the exciting laser line. It should be mentioned that excitation around 2.10 eV also leads to an enhanced PL of self-trapped CT2 states which additionally contribute to the PL intensity and spectral width of the low-energy band at  $\sim 1.69$  eV. Eventually, this band is composed of nonresolved CT1 and Frenkel exciton sub-

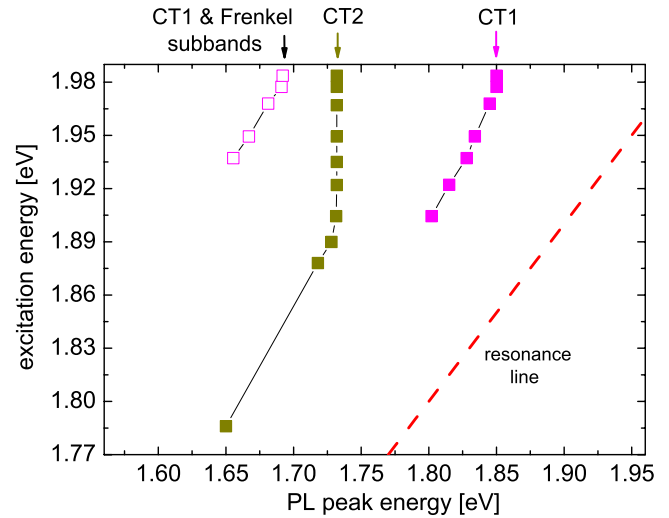


FIG. 6. (Color online) Different exciton emission channels of a 90-nm-thick PTCDA film at 5 K as a function of the excitation energy ranging from 1.786 to 1.983 eV. The energetic positions of the CT1 and CT2 transitions are obtained from the spectra in Fig. 5 by a multi-Gaussian line-shape analysis. The dashed-red line is showing the position of emission resonant with the excitation energy.

bands as well as of the PL band of CT2 states generated by the relaxation of CT2-nr states into self-trapped CT2 excitons.

## B. PTCDA polycrystalline films

Figure 5 shows the PL spectra of a 90-nm-thick PTCDA polycrystalline film on Si(100) substrate at 10 K at various excitation energies ranging from 1.889 to 1.983 eV and at a laser power of  $\sim 100$   $\mu\text{W}$ . The spectra are normalized and offset to each other for better comparison. Furthermore the PL using the Ar-ion laser line at 2.411 eV as excitation source is given as the topmost spectrum. In addition, Fig. 5 contains the PL spectra obtained at excitation energies of  $\sim 1.88$  and  $\sim 1.79$  eV that were provided by GaAs semiconductor lasers. As in the previous investigations on PTCDA crystals the center energies of the emission bands were determined from the spectra in Fig. 5 using multi-Gaussian functions where the spectral position of the CT2 Gaussian was kept fixed above an excitation of 1.90 eV in order to obtain a higher accuracy of the CT1 and CT1-subband energies as visualized in Fig. 6.

Similar to the analysis of the PL bands observed on a PTCDA crystal displayed in Fig. 2, Fig. 6 demonstrates that also in thin films the self-trapped CT2 PL appears at the lowest-excitation energies. As already mentioned, our exciton model displayed in Fig. 1 does not provide any excitation resonance in that energetic region. We therefore assign the lowest PLE resonance again to specific defects at lower-energy favoring charge separation into anion-cation pairs resulting in a broad PL band of self-trapped CT2 excitons.<sup>29</sup> The contribution of the CT2 transition relative to the CT1 transition is higher in the polycrystalline PTCDA film as compared to the PTCDA crystal which might be explained

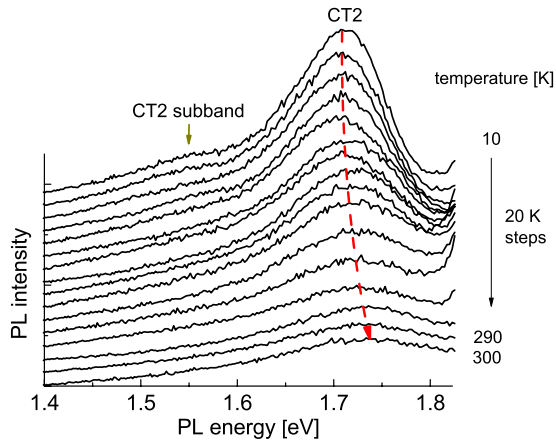


FIG. 7. (Color online) Temperature-dependent PL of CT2 and vibronic CT2-subband states obtained from a 50-nm-thick PTCDA film at an excitation energy of 1.878 eV. The temperature is varied in the range between 10 and 300 K in 20 K steps as labeled. The red dashed arrow connecting the emission maxima is a guide to the eye.

by an increased density of defect-related CT2 states that are preferentially formed by slightly deformed or compressed stacked PTCDA molecules in the vicinity of defects or at grain boundaries.<sup>23</sup>

The CT2 emission intensity decreases above  $\sim 1.9$  eV excitation energy and reveals a constant peak energy of  $\sim 1.73$  eV, showing that the laser energy starts to exceed the maximum of the density of absorbing states resulting preferentially in PL from self-trapped CT2 excitons. At the excitation energies of 1.878 and 1.786 eV we find a redshift of the CT2 emission band demonstrating that the GaAs laser lines excite CT2 states which are lying below the distribution maximum. While it is not possible to compare the PL intensities obtained at the energies of the GaAs laser and of the DCM laser, the relative intensities between the 1.878 and 1.786 eV spectra show a reduction by a factor of  $\sim 10$ . The PL blueshift indicates that the CT2 PLE resonance occurs at  $\sim 1.89$  eV, in agreement to our investigations on PTCDA crystals.

Due to the high selectivity of the CT2 transition at an excitation energy of 1.88 eV we further performed temperature-dependent PL measurements ranging from 10 to 300 K which are shown in Fig. 7. At low temperatures (10 K) the CT2 emission is composed of the main band at 1.71 eV and a further vibronic subband at  $\sim 160$  meV lower energy. These very broad PL features demonstrate that self-trapping along the stacking direction and other symmetry-lowering distortions contributing to the broadening are essential features of this specific radiative recombination.<sup>29</sup> Together with the very long recombination time discussed earlier, a monomolecular recombination mechanism assigned to a specific impurity can safely be ruled out.<sup>12,13</sup>

With rising temperature both features shift to higher energies, and above  $\sim 100$  K due to increased thermal broadening both structures merge into an extended low-energy tail below the main peak. These features are attributed to a shift of the CT2 excitation resonance due to an increasing population of excited levels of low-frequency vibronic modes. These modes are responsible for an increasing broadening of

the CT2 transition,<sup>13,14</sup> thermal expansion of the lattice, and a small blueshift of the CT2 transition expected from a reduced Coulomb attraction at larger intermolecular distance. At room-temperature PTCDA has a thermal-expansion coefficient in the range between  $1.05 \times 10^{-4}$  and  $1.24 \times 10^{-4} \text{ K}^{-1}$ .<sup>34</sup> From studies of the lattice constant of other perylene pigments below room temperature<sup>33</sup> it can be concluded that the reduction in the stacking vector  $a$  in PTCDA at low temperature ( $\sim 10$  K) is in the range of about 1.5%. Together with the calculated dependence of the CT2 transition in PTCDA as a function of stacking vector  $a$  with  $dE_{\text{CT2}}/da = 0.5 \text{ eV}/\text{\AA}$  (Ref. 29) this indicates a blueshift of the CT transition of  $\sim 30$  meV when heating the sample from 5 K to room temperature, as observed in Fig. 7.

For the spectra obtained at 50 K, a line-shape analysis using a two-Gaussian fit according to Eq. (1) reveals a FWHM of  $\sim 120$  meV for the zeroth vibronic CT2 band and of  $\sim 155$  meV for its first vibronic subband. The vibronic coupling constant  $g^2$  given by the area ratio of the CT2 band and its subband  $a_1/a_0$  is found to be  $\sim 0.46$ . Both the obtained FWHM values as well as the coupling constant are close to values that have been obtained from previous PL measurements.<sup>13</sup>

At excitation energies higher than 1.89 eV the CT1 band appears in the PL spectra (see Figs. 5 and 6) of the PTCDA film. As in the PTCDA crystal the PL energy shows a blueshift that eventually reaches a constant emission energy of 1.85 eV at an excitation energy of 1.975 eV or above. Also the CT1 band is accompanied by its CT1 vibronic subband at  $\sim 160$  meV lower energy showing the same excitation energy dependence as the zero-order vibronic band. In accordance to our investigations in PTCDA crystals we conclude that the transition energy of the CT1 state in the nondeformed periodic crystal has its distribution maximum at  $\sim 1.98$  eV.

## VI. SUMMARY

Applying PLE spectroscopy at 5 K, we have studied the emission of selectively excited CT2, CT1, and CT2-nr states as well as of Frenkel excitons in PTCDA single crystals and PTCDA polycrystalline films. For the PTCDA single crystals the excitation energy ranged from 1.878 to 2.149 eV. With increasing excitation energy, subsequently the CT2, CT1, and CT2-nr bands emerge in the PLE spectrum. In addition a low-energy PL band at  $\sim 160$  meV below the main peak of the CT1 band is identified as a vibronic subband of the CT1 transition. When the laser starts to excite the low-energy tail of the different inhomogeneously broadened absorption resonances we find a blueshift with increasing excitation energy. As several of the mechanisms for spectral diffusion discussed for other organic materials cannot contribute in PTCDA, we conclude that reduced excitation energies in compressively strained regions are responsible for this effect. The blueshift saturates when the laser excitation energy exceeds the distribution maximum of the absorbing CT states, resulting in PL bands at different constant emission energies arising from different excited states. Furthermore the PLE signal intensity of each CT band reaches a maximum when



the exciting laser energy is resonant with the maximum of the individual state distribution in the equilibrium geometry of the crystal. From these observations we deduce the resonant absorption energies of the CT2, CT1, and CT2-nr PL bands to be  $\sim 1.89$ ,  $1.98$ , and  $2.10$  eV. The energy difference between the absorption and emission energy for the CT1 transition of  $\sim 110$  meV is explained by the Stokes shift of low-energy internal vibrations and external phonon modes. The larger energy difference of  $\sim 175$  meV for the CT2 transition is attributed to self-trapping of the anion-cation pairs along the stacking direction, resulting in an additional Stokes shift of  $\sim 65$  meV.

Comparing the measured excitation resonances of the CT PL bands with the exciton dispersion branches obtained from a model accounting for Frenkel excitons and CT states on stack neighbors,<sup>17</sup> the PLE investigations place the lowest resonant CT2 excitation 50 meV below the lowest-calculated CT2 state at the  $\Gamma$  point of the Brillouin zone, so that this excitation resonance cannot be assigned without assuming defect-related CT2 states favoring a charge separation. Since any localized defect such as a grain boundary or a stacking fault destroys the crystal periodicity, the  $\mathbf{k}$ -space picture for the excitonic dispersion breaks down. This allows exciting excitonic states at energies which do not correspond to the  $\Gamma$  point of the Brillouin zone but merely to a different region of  $\mathbf{k}$ -space, so that according to Fig. 1, states about 30 meV below the dispersion maximum at  $\Gamma$  may contribute. Therefore, the major part of the energetic difference of about 50 meV between calculated and measured  $E_{00}^{\text{CT2}}$  PLE resonance

energies seems to arise from a violation of the  $\mathbf{k}$ -space selection rule close to defects so that only a small fraction has to be assigned to compressive strain.

Moreover, the PLE experiments reveal that PL from CT1 states involving both basis molecules can be excited resonantly at  $\sim 1.98$  eV, or 30 meV above the position of the lowest calculated CT2 sublevel. For energies larger than  $\sim 2.04$  eV the indirect Frenkel exciton and CT2-nr occur in the PL spectra. In comparison with the model calculations the mixed Frenkel-CT2 states at an energy of  $\sim E_{01}^{\text{CT2}} = 2.12$  eV are the relevant excitation channels of the CT2-nr PL band. Unlike the CT states, the indirect Frenkel exciton emission occurring shows a much weaker blueshift when the PL excitation energy approaches the respective resonance from the low-energy side.

The PLE measurements on polycrystalline PTCDA films confirm previous assignments of the excitonic transitions in the PTCDA crystal. The contribution of the CT2 transition in the PLE spectra is larger in PTCDA films, which is attributed to an increased density of defect-related CT2 states that are preferentially excited in the vicinity of grain boundaries. Temperature-dependent measurements of these selectively excited CT2 transitions reveal a CT2 subband at  $\sim 155$  meV lower energy at 10 K. With increasing temperature the CT2 transition shifts by  $\sim 30$  meV to higher energies and the broadening increases due to the population of higher vibronic levels of the low-frequency modes in the excited state potential.

\*Present address: Department of Physics, University of Alberta, Edmonton, Alberta, Canada T6G2G7.

<sup>1</sup>H. Bässler and B. Schweitzer, *Acc. Chem. Res.* **32**, 173 (1999).

<sup>2</sup>A. Piaggi, G. Lanzani, G. Bongiovanni, A. Mura, W. Graupner, F. Meghdadi, G. Leising, and M. Nisoli, *Phys. Rev. B* **56**, 10133 (1997).

<sup>3</sup>U. Rauscher, H. Bässler, D. D. C. Bradley, and M. Hennecke, *Phys. Rev. B* **42**, 9830 (1990).

<sup>4</sup>N. T. Harrison, D. R. Baigent, I. D. W. Samuel, R. H. Friend, A. C. Grimsdale, S. C. Moratti, and A. B. Holmes, *Phys. Rev. B* **53**, 15815 (1996).

<sup>5</sup>R. G. Della Valle, E. Venuti, L. Farina, A. Brillante, M. Masino, and A. Girlando, *J. Phys. Chem. B* **108**, 1822 (2004).

<sup>6</sup>G. Salvan, D. Tenne, A. Das, T. U. Kampen, and A. R. T. Zahn, *Org. Electron.* **1**, 49 (2000).

<sup>7</sup>R. Scholz and M. Schreiber, *Chem. Phys.* **325**, 9 (2006).

<sup>8</sup>V. Bulović, P. E. Burrows, S. R. Forrest, J. A. Cronin, and M. E. Thompson, *Chem. Phys.* **210**, 1 (1996).

<sup>9</sup>S. R. Forrest, *Chem. Rev.* **97**, 1793 (1997).

<sup>10</sup>U. Gómez, M. Leonhardt, H. Port, and H. C. Wolf, *Chem. Phys. Lett.* **268**, 1 (1997).

<sup>11</sup>M. Leonhardt, O. Mager, and H. Port, *Chem. Phys. Lett.* **313**, 24 (1999).

<sup>12</sup>A. Y. Kobitski, R. Scholz, I. Vragović, H. P. Wagner, and D. R. T. Zahn, *Phys. Rev. B* **66**, 153204 (2002).

<sup>13</sup>A. Y. Kobitski, R. Scholz, D. R. T. Zahn, and H. P. Wagner,

*Phys. Rev. B* **68**, 155201 (2003).

<sup>14</sup>H. P. Wagner, A. DeSilva, and T. U. Kampen, *Phys. Rev. B* **70**, 235201 (2004).

<sup>15</sup>M. Schneider, E. Umbach, and M. Sokolowski, *Chem. Phys.* **325**, 185 (2006).

<sup>16</sup>H. P. Wagner, A. DeSilva, V. R. Gangilenka, and T. U. Kampen, *J. Appl. Phys.* **99**, 024501 (2006).

<sup>17</sup>L. Gisslén and R. Scholz, *Phys. Rev. B* **80**, 115309 (2009).

<sup>18</sup>M. Möbus, N. Karl, and T. Kobayashi, *J. Cryst. Growth* **116**, 495 (1992).

<sup>19</sup>Z. G. Soos, M. H. Hennessy, and G. Wen, *Chem. Phys.* **227**, 19 (1998).

<sup>20</sup>M. Hoffmann and Z. G. Soos, *Phys. Rev. B* **66**, 024305 (2002).

<sup>21</sup>M. H. Hennessy, Z. G. Soos, R. A. Pascal, and A. Girlando, *Chem. Phys.* **245**, 199 (1999).

<sup>22</sup>M. H. Hennessy, R. A. Pascal, and Z. G. Soos, *Mol. Cryst. Liq. Cryst.* **355**, 41 (2001).

<sup>23</sup>V. R. Gangilenka, A. DeSilva, H. P. Wagner, R. E. Tallman, B. A. Weinstein, and R. Scholz, *Phys. Rev. B* **77**, 115206 (2008).

<sup>24</sup>I. Vragović, R. Scholz, and M. Schreiber, *Europhys. Lett.* **57**, 288 (2002).

<sup>25</sup>I. Vragović and R. Scholz, *Phys. Rev. B* **68**, 155202 (2003).

<sup>26</sup>R. Scholz, I. Vragović, A. Yu. Kobitski, M. Schreiber, H. P. Wagner, and D. R. T. Zahn, *Phys. Status Solidi B* **234**, 402 (2002).

<sup>27</sup>R. Scholz, M. Schreiber, I. Vragović, A. Y. Kobitski, H. P. Wag-

- ner, and D. R. T. Zahn, *J. Lumin.* **108**, 121 (2004).
- <sup>28</sup>H. P. Wagner, V. R. Gangilenka, A. DeSilva, H. Schmitzer, R. Scholz, and T. U. Kampen, *Phys. Rev. B* **73**, 125323 (2006).
- <sup>29</sup>R. Scholz, A. Y. Kobitski, D. R. T. Zahn, and M. Schreiber, *Phys. Rev. B* **72**, 245208 (2005).
- <sup>30</sup>M. I. Alonso, A. Garriga, N. Karl, J. O. Osó, and F. Schreiber, *Org. Electron.* **3**, 23 (2002).
- <sup>31</sup>A. Djurisić, T. Fritz, and K. Leo, *Opt. Commun.* **183**, 123 (2000).
- <sup>32</sup>M. I. Alonso, A. Garriga, J. O. Osó, F. Schreiber, L. Gisslén, and R. Scholz (unpublished).
- <sup>33</sup>J. Mizuguchi and K. Tojo, *J. Phys. Chem. B* **106**, 767 (2002).
- <sup>34</sup>B. Krause, A. C. Duerr, F. Schreiber, H. Dosch, and O. H. Seeck, *J. Chem. Phys.* **119**, 3429 (2003).
- <sup>35</sup>M. Hoffmann, K. Schmidt, T. Fritz, T. Hasche, V. M. Agranovich, and K. Leo, *Chem. Phys.* **258**, 73 (2000).
- <sup>36</sup>E. V. Tsiper and Z. G. Soos, *Phys. Rev. B* **64**, 195124 (2001).
- <sup>37</sup>G. Mazur and P. Petelenz, *Chem. Phys. Lett.* **324**, 161 (2000).
- <sup>38</sup>U. Heinemeyer, R. Scholz, L. Gisslén, M. I. Alonso, J. O. Osó, M. Garriga, A. Hinderhofer, M. Kytka, S. Kowarik, A. Gerlach, and F. Schreiber, *Phys. Rev. B* **78**, 085210 (2008).
- <sup>39</sup>V. Bulović and S. R. Forrest, *Chem. Phys.* **210**, 13 (1996).